NASA Technical Memorandum **107660**

Transient / Structural Analysis of a Combustor under Explosive Loads

Peyton B. Gregory
Anne D. Holland

December 1992

National Aeronautics and
Space Administration

Langley Research Center
Hampton, Virginia 23665-5225

Table of Contents

List of Figures

List of Tables

List of Symbols

f = frequency

f_h = capacity of hook in concrete

f_L = frictional resistance of bolt in concrete

k_1 = thrust anchor stiffness

k_2 = pressure shell stiffness

m = tunnel mass

p_{bal} = equilibrium pressure on nozzle

p_{cp} = pressure on closure plug

p_{nozz} = pressure on nozzle

p_{shell} = pressure on combustor shell

t_{fd} = time for flame-out detection

t_L = time lag from flame-out to fuel valve closed

t_s = time for shut down

C_i = fuel concentration

G = control system gains

K = stiffness matrix

KG = geometric stiffness matrix

KGG = K+KG

L = length

M_a = mass flow of air

M_{eq} = equivalent fuel mass

M_f = mass flow of fuel

P = pressure

P_e = measured pressure

P_i = pressure prior to flame-out

P_o = initial deflagration pressure

S_f = turbulent burning velocity

S_u = laminar burning velocity

T = temperature

T_e = measured temperature

T_i = temperature prior to flame-out

U = mean flow velocity

$V_{f,up}$ = upstream flame velocity

α = ratio of turbulent burning velocity to laminar burning velocity

δ = deflection

σ = stress

υ_b = specific volume of burned material

υ_u = specific volume of unburned material

1.0 Introduction

The 8-Foot High Temperature Tunnel (HTT) at NASA Langley Research Center is a combustion-driven blow-down wind tunnel. The 8 foot diameter by 12 foot long free jet test section is designed to achieve Mach 4, 5, and 7 with true temperature simulation. The combustor has two primary modes of operation: (1) methane and air, and (2) methane and air with oxygen enrichment to raise the combustion products oxygen content to 20%. The first mode of operation is used for aerothermal loads testing and flight weight structural concept verification; the second mode is used to test air breathing scramjet and ramjet engines.

A major potential failure mode that was considered during the combustor redesign was the possibility of a deflagration and/or detonation in the combustor. If a main burner flame-out were to occur, then unburned fuel gases could accumulate and, if reignited, an explosion could occur. The current system includes sensors that are designed to detect a flame-out and initiate shut down procedures. The time between flame-out, detection, and shut down determines the amount of fuel available for an explosion and therefore is the critical parameter in limiting the potential energy associated with an explosion.

The objective of this evaluation is to determine the safe operating limits of the combustor under transient explosive loads to prevent a catastrophic failure of the pressure boundary. To accomplish this, a detailed transient, structural finite element analysis of the combustor system (end closure plug, pressure shell, combustor nozzle, tunnel mass and thrust anchor) was performed using PATRAN (ref. 1) model development and EAL (ref. 2) analysis software. The critical failure mechanisms were identified, and the maximum allowable deflagration pressure versus equivalent fuel mass was determined. This information can then be used to bound the allowable equivalent fuel mass and combustor pressure parameters for various shut down times coupled with various combustion-process control system parameters.

1.1 Analysis Process

The analysis process and interactions are shown in figure 1. One of the key elements in the process is the control system math model which is a simulation of the control system and how the combustor responds to the system control parameters. The math model results are compared and correlated to test data to accurately reflect the actual conditions. The math model then provides the necessary parameters to determine equivalent fuel mass which is then used as input to the gas dynamics analysis. In addition, flammability, ignitability, flame propagation, detonation structure, and chemical kinetics are integrated into the gas dynamics analysis for a particular test condition. The gas dynamics analysis results are then integrated into the combustor transient structural dynamics analysis. From this analysis, the structural dynamic evaluation is performed, and structural frequency sensitivity is assessed. Finally, integrating a structural failure criteria with the structural dynamic results establishes the performance limits of the combustor. The gas dynamics analysis is covered briefly while the failure criteria, failure mechanisms, and the structural dynamic analysis are covered in detail.

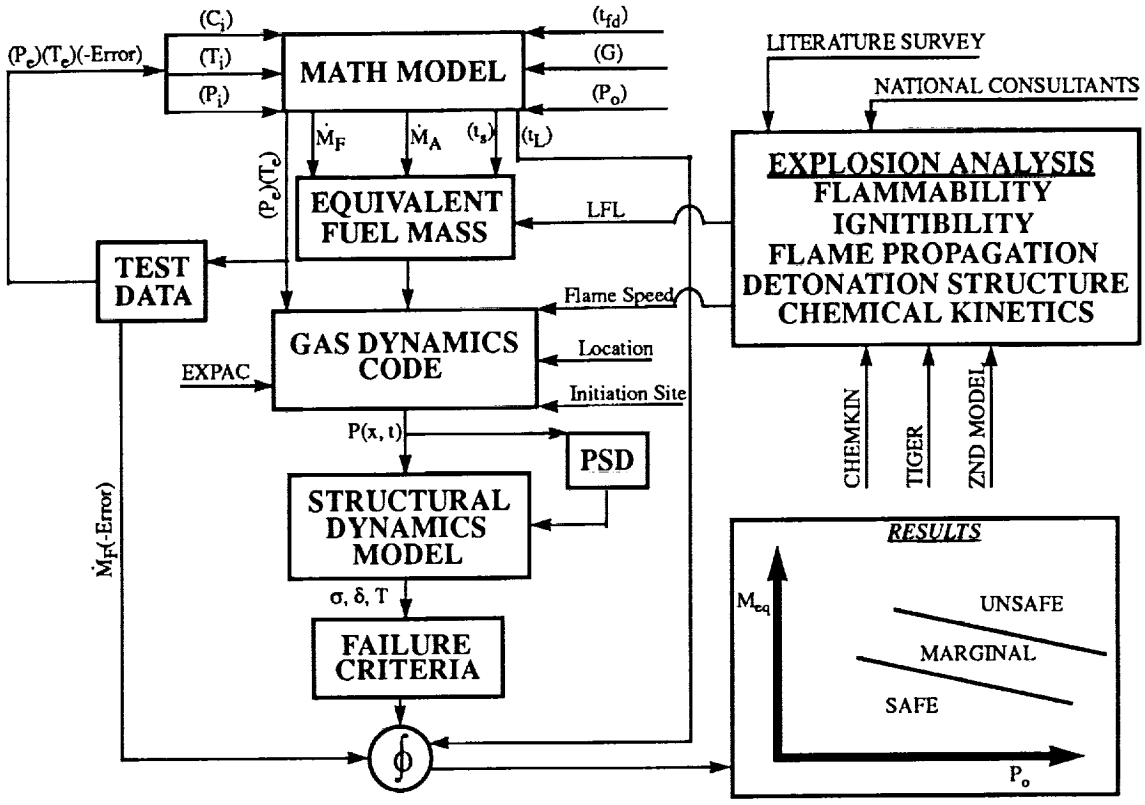

Figure 1. Analysis Process.

2.0 Component Description

The combustor system, including the nozzle, pressure shell, and end closure plug, is shown in figure 2. The nozzle is transpiration cooled, consisting of four housings and 15 platelet stacks. The nozzle is secured to the pressure shell by 12 keyed segments bolted to the housing. The pressure shell is 30 feet long and is constructed from three main components; the main barrel section and the two forged barrel ends. The main barrel is 134.25 inches long and has an inner diameter of 44.5 inches. It is a laminated plate structure consisting of one 0.5 inch layer and sixteen 0.25 inch layers with a total thickness of 4.5 inches. The barrel ends are machined forgings with full penetration welds to the main barrel. The closure plug is a quick-actuating mechanism which assists easy removal to facilitate inspection of the combustor internals. It consists of several segmented rings and interlocking circumferential keys. The entire tunnel is supported in the axial direction by the thrust anchor which is located at the down stream end of the transpiration cooled nozzle. Table 1 summarizes the material properties for the combustor's primary structural components.

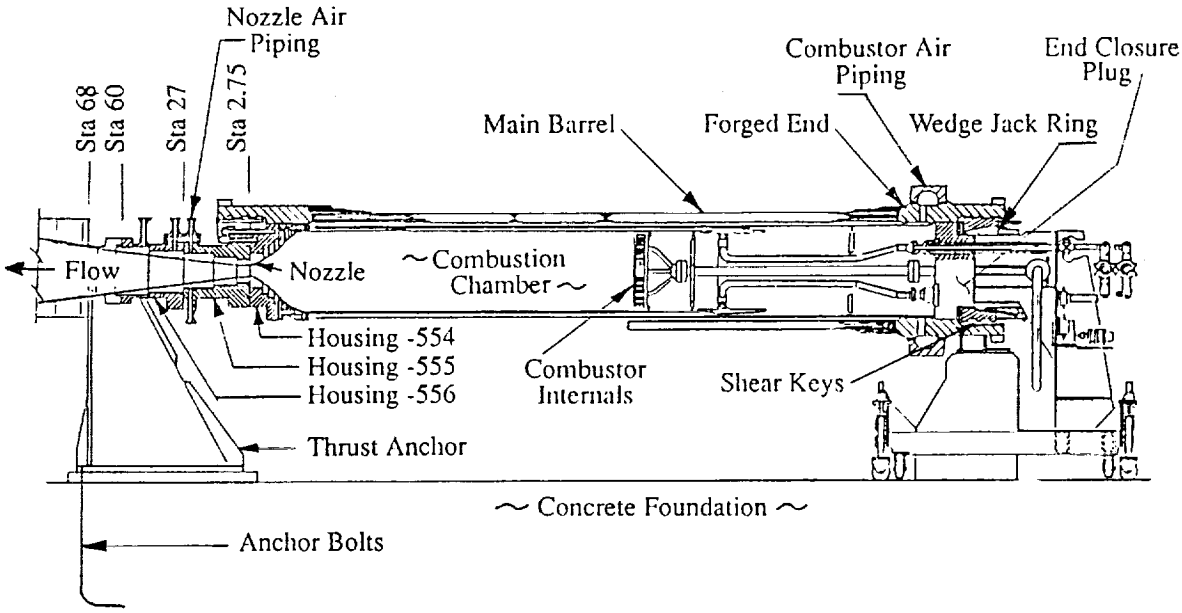

Figure 2. 8 Foot High Temperature Tunnel Combustor Configuration.

Table 1. Combustor System Primary Structural Component Material Properties.

Component	Material	Tensile Strength (ksi)	Yield Strength (ksi)
Main Barrel	A225-C	105.0	70.0
Forged Ends	SA-105	70.0	36.0
Housing -556	SA-336(304L)	65.0	25.0
Housing -554, -555	SA-336(C1.F304)	70.0	30.0
Bolts (Sta 60, 27, 2.75)	SA-354 Gr BD	150.0	130.0
Pressure Shell (Sta 68)	SA-182 F347	70.0	30.0
Thrust Anchor	A36	58.0	36.0
Anchor Bolts	A36	58.0	36.0
Concrete Foundation	Ultimate Compressive Strength = 3000.0 psi		

3.0 Failure Criteria

The structural criteria used to evaluate the combustor components was chosen to prevent catastrophic failure of any component in the combustor system. Specifically, catastrophic failure is defined as a failure which would result in a potential personnel hazard which includes a penetration of the pressure boundary or the failure of the thrust anchor. Therefore, the components considered in this analysis are those which actively contain pressure and the components of the thrust anchor. The strength values used in determining the allowable stresses are the minimum published values. The stress evaluation criteria, in addition to the other evaluation criteria used to evaluate the combustor system, are defined in table 2.

Table 2. Combustor Structural Component Failure Criteria.

Description	Criteria
1. Prevent catastrophic failure of the pressure boundary;	$\sigma_{max} \leq$ the lesser of, 1.33 Yield Strength or Ultimate Strength
2. Barrel displacement at shear keys;	$\delta_{max} \leq$ 1/10 (shear key depth) = .13 inches
3. Combustor air piping displacement;	$\delta_{max} \leq$ 2.0 inches
4. Nozzle air piping displacement;	$\delta_{max} \leq$ .5 inches
5. Tunnel displacement;	$\delta_{max} \leq$ .25 inches

The first criteria is typically used in industry for the ductile failure analysis of pressure vessel explosions. This criteria is extended in this study to evaluate all critically stressed components and was found to be the controlling criteria. The remaining criteria (2-6 table 2) are not failure criteria but are functional criteria to ensure no problems occur in these areas. The second criteria precludes the barrel from displacing and disengaging the shear keys. One-tenth the shear key depth was conservatively chosen to eliminate additional stress considerations such as large displacement bending. The third criteria precludes over stressing the combustor air piping. When the nozzle components are assembled or disassembled, the combustor is displaced approximately 2 inches which similarly displaces the combustor air piping. Therefore, the 2 inch maximum displacement criteria is a field tested criteria. The fourth criteria prevents over stressing the nozzle air piping. During assembly, the piping can be adjusted approximately 1/2 inch for alignment with the nozzle; thus, this value is conservatively set as a limiting criteria for the nozzle piping. The fifth criteria limits overstressing tunnel components down stream of the thrust anchor. A jacking system located between the thrust anchor and the test section is used to exchange tunnel components and has a minimum travel distance of 1/4 inch. Therefore a 1/4 inch criteria was used to ensure all thrust loading is taken out at the thrust anchor.

4.0 Failure Loading Mechanisms

There are two main failure loadings: (1) peak pressure and (2) differential pressure. The peak pressure introduces loads to the laminated barrel, the forged ends, and the end closures. The differential pressure (or thrust loads) introduces gross tension or shear in all components up to the thrust anchor.

4.1 Peak Pressure Loading

The peak pressure loading develops a hoop stress in the laminated barrel and the forged ends. Using the material properties from table 1, the maximum allowable stresses for the laminated barrel and the forged ends are determined from criteria 1, table 2. The values of the allowable stresses that are used to evaluate the stress results for the laminated barrel and the forged ends are shown in table 3.

Table 3. Allowable Hoop Stress on the Combustor Shell.

Component	Material	Allowable stress, ksi
Laminated Barrel	A225-C	93.0
Forged Ends	SA-105	47.0

The peak pressure load on the end closures transfers load into the shear keys, the pressure shell, and the wedge jack ring. Table 4 gives the allowable load on the components which must resist peak pressure on the end closures.

Table 4. Allowable Load from Peak Pressure on End Closure Component.

Component	Material	Allowable Stress, ksi	Area in^2	Allowable Load $x10^6$ lbs
Shear Keys	SA-105	23.9	1187.5	28.3 - shear
Shell/Forging	SA-105	47.9	765.8	35.9 - tension
Shell/Laminate	A225-C	93.1	692.7	64.4 - tension
Wedge Jack Ring	SA-354 Gr BD	150.0	8.4	1.26 - tension

4.2 Differential Pressure Loading

There are two main components which must withstand the thrust loading. First is the thrust anchor in which bending and shear of the structure and tension in the anchor bolts is of concern. And secondly is the nozzle and combustor components in a state of gross tension or shear.

4.2.1 Thrust Anchor

A schematic of the thrust anchor and bolt pattern are shown in figure 3. There are 28 two inch diameter anchor bolts with an effective cross-sectional tensile area of 2.50 in^2 per bolt. The entire thrust anchor was analyzed to determine the maximum bending stress and the maximum shear stress. In addition, the capacity of the anchor bolts and the concrete were determined.

The maximum bending stress occurred at section 1 (see figure 3) and the maximum shear stress occurs at section 2. To determine the maximum stress in the anchor bolts, several iterations were made to match the edge of the contact compression area with the section centroid. The anchor bolts are embedded in concrete 42.0 inches deep with a 12 inch hook at the end. There are two components which contribute to the strength of the anchor bolt in the concrete (ref. 3). First is the frictional resistance over the embedded length of the bolt f_L, and second is the capacity of the hook f_h. The allowable stresses are based on criteria 1, table 2; and the results are shown in table 5.

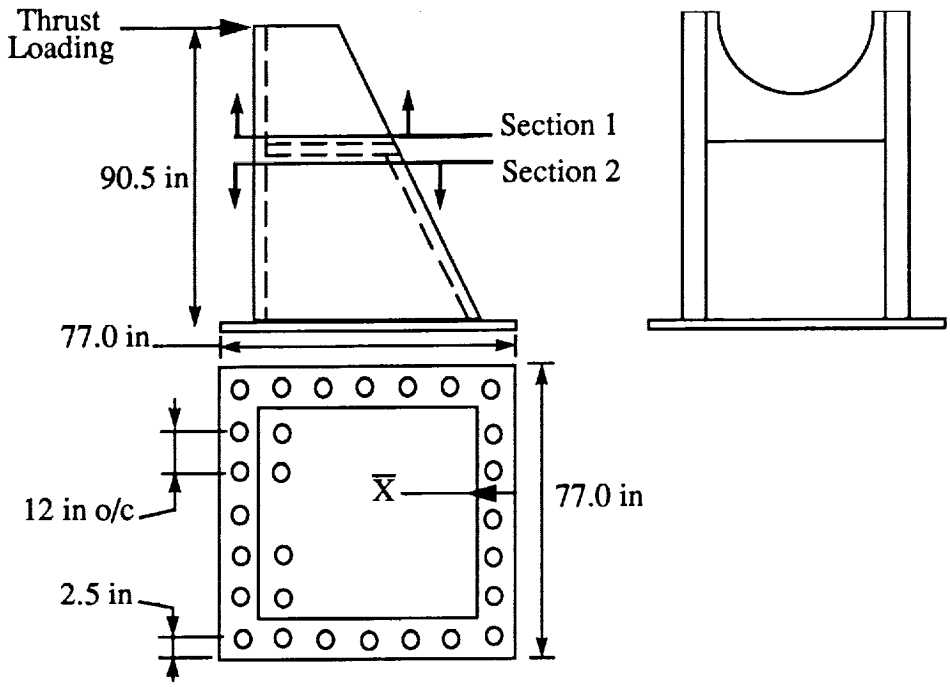

Figure 3. Thrust Anchor

Table 5. Allowable Thrust Anchor Loads.

Component	Allowable Load, lbs
Section 1	1.30×10^6 - bending
Section 2	1.84×10^6 - shear
Anchor Bolts	1.20×10^6 - tension
Concrete	1.00×10^6 - pull out

The capacity of the anchor bolts in the concrete is the controlling factor which limits the overall capacity of the thrust anchor to 1.07×10^6 lbs. The capacity of the anchor bolts in the concrete was also determined by another method which considered a cone of failure in the concrete using the capacity of concrete in tension. These results indicate a maximum allowable thrust load of 1.00×10^6 lbs which agrees well with 1.07×10^6 lbs from the initial analysis. The lower value of 1.00×10^6 lbs is used to evaluate the thrust loads.

4.2.2 Nozzle and Combustor Components

Table 6 defines the allowable thrust load on the components which must withstand the unbalanced pressure loading (thrust loading). Since for each component the material is known, then the allowable load is equal to the allowable stress times the cross sectional area of the component.

Table 6. Allowable Thrust Load from Unbalanced Pressure Loads.

Component	Material	Allowable Stress, ksi	Area in^2	Allowable Load $x10^6$ lbs
Sta. 68/Shell	SA-182 Gr F347	39.9	50.80	2.027 - tension
Sta. 60/Bolts	SA-354 Gr BD	150.0	27.27	4.158 - tension
Housing -556	SA-336 304L	33.2	82.55	2.740 - tension
Sta. 27/Bolts	SA-354 Gr BD	150.0	71.20	10.68 - tension
Housing -555	SA-336 C1.F304	39.9	246.3	9.826 - tension
Sta. 2.75/Bolts	SA-354 Gr BD	150.0	69.36	10.404 - tension
Housing -554	SA-336 C1.F304	19.9	361.2	7.206 - shear

5.0 Blast Wave Loadings

The spatial and temporal distribution of pressure within the combustor was determined (ref. 4) using inputs from the control system math model. An overview of the analysis follows.

The major concern with the combustor is if it were running under normal conditions and a flame-out occurred. This would result in an accumulation of combustion gases and, if re-ignited, an explosion could occur. The types of explosions and the parameters required for an explosion to occur are explained in the following sections.

5.1 Explosion Scenarios

There are three basic explosion scenarios: (1) deflagration, (2) deflagration to detonation transition (DDT), and (3) a direct detonation. A deflagration is characterized by subsonic flame speeds and can be initiated by low energy sources. A direct detonation is characterized by supersonic flame speeds and requires a high energy ignition source. A DDT is characterized by an initial deflagration in which the flame speed increases to a critical speed which initiates a detonation.

Preliminary assessments indicated that the combustor could not safely contain any level of a DDT and that the combustor can only safely contain a low-level deflagration. Therefore, the main consideration in this analysis was to determine the maximum level of deflagration that the structure could withstand using the failure criteria in table 2.

5.2 Flammability

The flammability of the mixture downstream of the spray bar is determined by three factors: (1) composition, (2) temperature, and (3) pressure. The composition of the natural gas supplied to the facility is generally 90-96% methane with the remaining mixture consisting of propane, ethane, nitrogen and other trace elements. The natural gas is then compressed to 6000 psi which liquefies the propane leaving a mixture of 98% methane and 2% ethane. The ethane content has a negligible effect on the thermochemical properties of the mixture as compared with pure methane. At the flammability limits, the

adiabatic flame temperature for a wide variety of fuel-oxidizer systems is approximately 1400°K (ref. 5).

One of the key combustion parameters is the Lower Flammability Limit (LFL). This value is the percent methane by volume at which the mixture becomes flammable.

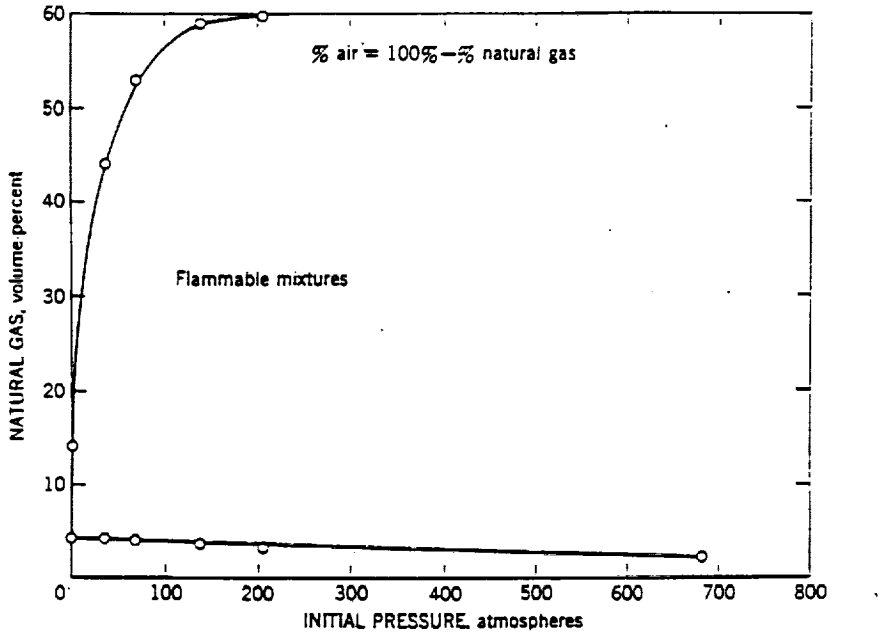

Figure 4. Effect of pressure on flammability limits of natural Gas at 28° C.

Figure 4 is a plot of Natural Gas Volume (%) versus Initial Pressure (atmospheres) showing the area of flammable mixtures (ref. 6).

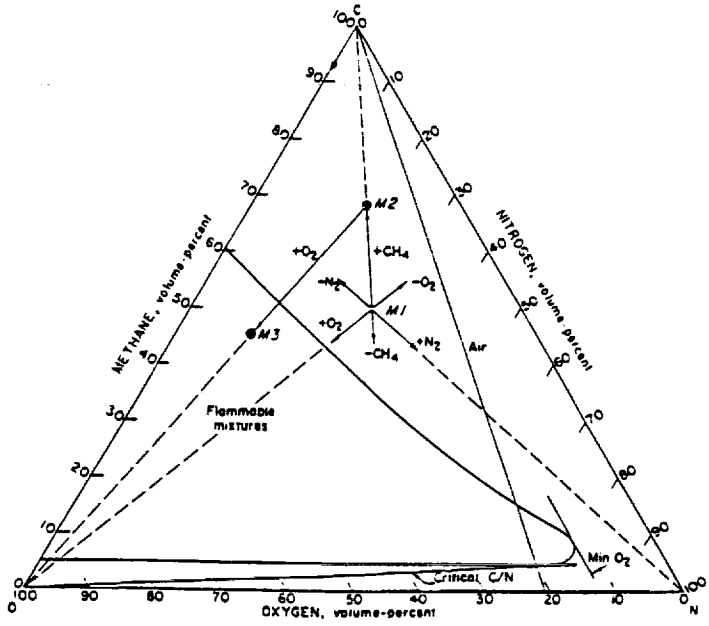

Figure 5. Flammability diagram for the Methane-Oxygen-Nitrogen system.

From figure 4, the LFL is determined to be approximately 5% and the LFL is found to be relatively insensitive to initial pressure. A typical operating point for the combustor of 2000 psi is equal to 136 atmospheres.

Figure 5 is a plot of flammable mixtures in terms of the volume-percent of methane, nitrogen, and oxygen (O_2) (ref. 6). The figure shows that the O_2 content has little effect on the lower flammability limit and that the LFL is approximately 5% methane by volume.

5.3 Ignitability

There are three primary sources in the combustor environment which could ignite flammable gases after a flame out has occurred. First are the hot surfaces downstream of the spray bar. Any surface with a temperature exceeding 900-1200° K can be considered a potential ignition source. Since the combustion products are at a temperature of 2000° K, high surface temperatures on the liner and temperature probes are possible sources. Second is the turbulent mixing of hot combustion gases with the cool fuel-air mixtures. And finally is the electrical discharge due to static charges on particulates in the flow. Given the possibilities for ignition sources and mechanisms, ignition of flammable mixtures after a flame-out is likely.

All of the potential ignition sources are of a low energy level and are capable of initiating a deflagration but there are no energy sources high enough to initiate a direct detonation. Therefore the only explosion hazards associated with a flame-out would be either a deflagration or a DDT.

5.4 Flame Propagation

There are three primary issues concerning flame propagation: (1) the effect of nozzle venting, (2) the turbulent burning velocity of methane, and (3) flame propagation upstream. The effect of nozzle venting would be to produce a mean flow which can both augment and oppose the flame and to decrease the rate of pressure rise. Estimates of the venting parameter (ref. 7) for the combustor indicates that the throat area is small relative to the combustor volume and that the time duration is short enough such that overpressure reduction due to nozzle venting is negligible.

The turbulent burning velocity of methane, S_f, is related to the laminar burning velocity, S_u, by a scale factor α such that $S_f = \alpha(S_u)$. The laminar burning velocity is documented for pressures up to 90 atmospheres; S_u = .35 m/s at one atmosphere and S_u = .05 m/s at 90 atmospheres. The scale factor a has a wide range of values depending on the circumstances; α = 10 from self induced turbulence, α = 70 - 150 when combined with the reacted gas expansion displacement effects, and α = 2300 is the maximum observed ratio of turbulent to laminar velocity at atmospheric pressure. Table 7 gives a range of turbulent burning velocities relative to the scale factors, α, given above. The range is between .5 and 115 m/s. For the gas dynamics analysis, a range of between 10 and 200 m/s was chosen to bracket the effect of flame speed on the combustor structural system.

Table 7. Turbulent Burning Velocity of Methane, (S_f).

Laminar Burning Velocity S_u, m/s	Ratio of Turbulent to Laminar Velocity, α	S_f, m/s
.05	10	.5
.05	70	3.5
.05	150	7.5
.05	2300	115

The upstream flame velocity is given by; $V_{f,up} = (\upsilon_b/\upsilon_u)S_f - U$, where U is the mean flow velocity in the combustor, (υ_b/υ_u) is the expansion ratio, and S_f is the effective burning velocity. For the combustor, U is about 1 m/s and the expansion ratio is between 7 and 15. For upstream propagation the following must be satisfied; $(\upsilon_b/\upsilon_u)S_f > U$. Conservatively using the slowest flame speed in Table 7 (.5 m/s) and the smallest expansion ratio of 7, the inequality becomes, 3.5 > 1.0. Therefore upstream propagation is probable.

5.5 Equivalent Fuel Mass

Equivalent fuel mass is a convenient method to access the energy potential of a given quantity of fuel-oxidizer mixture. For the case under consideration, the control system math model is used to determine the fuel-oxidizer distribution in the combustor after an assumed flame out. Integration of the mass-energy for mixtures above the LFL defines the total available energy. This total energy is divided by the energy per unit mass of a stoichiometric mixture to yield the equivalent fuel mass.

5.6 Blast Wave Computations

The blast wave computations are accomplished through a series of calculations. The results from the control system math model of the combustor, which include combustor pressure, mass flow across the spray bar, and the mass flow of the methane as a function of time, are used as input variables in the model to estimate the spatial distribution of composition and the thermodynamic variables. Thermodynamic computations are then made using the STANJAN program (ref. 8) to obtain the change in energy for the lean combustion reaction. Finally the gasdynamic simulations are made using a Lagrangian solution of the inviscid one-dimensional compressible flow equations of an ideal gas. From the above, the spatial and temporal pressure distribution in the combustor ca be determined for various tunnel conditions.

6.0 Pressure Profiles

Figure 6 shows the pressure profile for 2.25 kg equivalent fuel mass and 200 m/s flame speed developed from the gas dynamics analysis. The three axes represent length, time, and normalized pressure. The length axis defines the pressure from the nozzle to the closure plug. The time axis runs out until the pressure waves have been sufficiently damped. The initial pressure, at time t=0, is defined as the initial deflagration pressure. If

the tunnel were running at a particular operation pressure and a flame-out occurred, the pressure field would decay until reignition occurred. The decayed pressure field is the initial deflagration pressure.

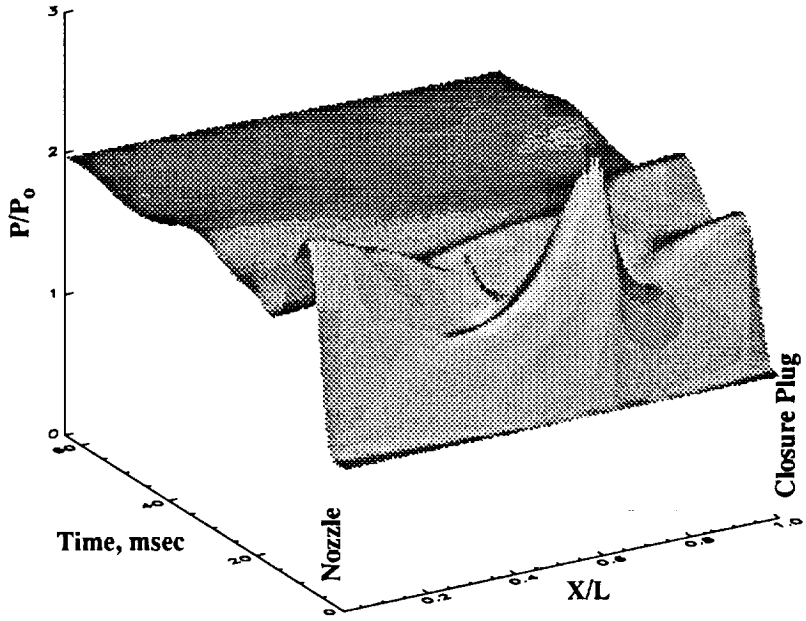

Figure 6. Pressure Profile for 2.25 kg Fuel and 200 m/s Flame Speed.

7.0 Finite Element Model

Figure 7 is a plot of the axisymmetric finite element model which includes details of the end closure plug, wedge and key segments, the pressure shell, and the nozzle components. In addition, there are spring and mass elements to account for the structure that connects the nozzle to the thrust anchor, the thrust anchor structure, and the mass of the remaining tunnel. There are nonlinear contact elements at the interface between each section such as flanged and keyed areas. The model is constrained in the axial direction at the thrust anchor. The bolts are modeled as axial rod elements at stations 27.25, -2.75, -16.0, (see figure 2) and connecting the keyed section to the nozzle. The bolt preloads are simulated by applying an appropriate negative temperature differential to the rod elements. There are 3939 grid points and 2217 elements in the model.

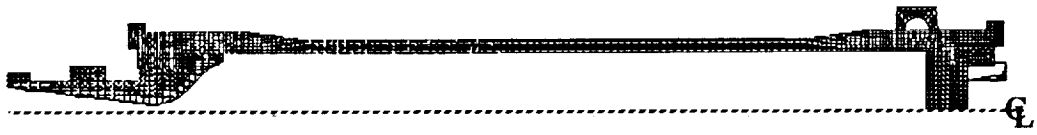

Figure 7. Finite Element Model of Combustor.

7.1 Loads

There are two basic loadings considered in the analysis. First is the combustor pressure histories, and second is the total thrust of the entire tunnel. Figure 8 shows how the loads are applied. The thrust anchor stiffness is represented by k_1, the pressure shell connecting the nozzle to the remaining tunnel is represented by k_2, and 'm' represents the remaining tunnel mass. The pressure histories are applied as p_{nozz}, p_{shell}, and p_{cp} which represent the pressures on the nozzle, shell, and closure plug, respectively. The total thrust can be represented by two components. First is the thrust from the combustor and second is the thrust from the remaining tunnel. The two thrust values were determined by closed form techniques. For the combustor thrust, p_{bal} is applied such that equilibrium is attained at initial conditions. For the remaining tunnel thrust, F_{tunnel} was applied to the tunnel mass 'm'. During the transient, p_{bal} and F_{tunnel} remained constant while p_{nozz}, p_{shell}, and p_{cp} vary with time.

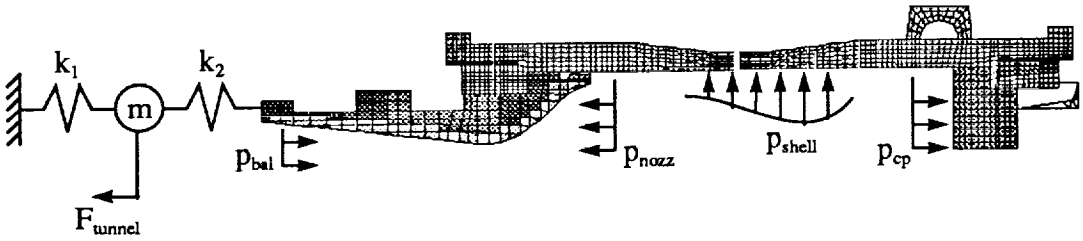

Figure 8. Finite Element Model Loads.

7.2 Load Cases

Thirteen different load cases are considered in the analysis. Table 8 shows the load cases and the variables that were considered. Flame speed is varied from 10 to 200 m/s to determine the sensitivity of the response to flame speed. Equivalent fuel mass was varied from 2.25 to 8 kg to determine the fuel-mass limits.

Table 8. Load Cases.

Table Values Indicate Initial Deflagration Pressures, P_o

Equivalent Fuel Mass	Flame Speed			
	10 m/s	50 m/s	100 m/s	200 m/s
2.25 kg	900 psi	900 psi	900 psi	900 psi 2000 psi 3000 psi
4 kg		900 psi	900 psi	900 psi 2000 psi 3000 psi
6 kg				900 psi
8 kg				900 psi

In addition, the initial deflagration pressure was varied to determine the accuracy of scaling results. The values in table 8 are initial deflagration pressures.

7.3 Analysis Procedure

The initial deflagration pressure is applied to the static model as a preload condition. Displacements and stresses from this preload are used to generate a geometric stiffness matrix, KG, which is then added to the original stiffness matrix, K. This new stiffness matrix, KKG = K+KG, is then used to calculate the natural modes of the system and in all further analyses. Once the modes are determined, participation factors are calculated and examined to determine how many modes should be used in the dynamic response analysis. For accuracy, 80 modes are used in the analysis, although about half that number (~40), would have been sufficient.

The pressure time histories are supplied at 142 even increments along the pressure shell between the closure plug and the nozzle. This data is interpolated to fit the axial locations along the pressure shell of the finite element model. The pressure at the last station near the closure plug end is used for the closure plug and the pressure at the last station near the nozzle is used for the nozzle.

For the analysis, unit pressures are applied to the shell, closure plug and nozzle. The equivalent nodal forces from the unit pressures are extracted and moved into an applied force data set where each block corresponded to a distinct axial location along the shell, the closure plug or the nozzle. The actual pressures versus time tables are shifted to a large matrix which is used along with the applied force data set to provide the amplitudes and forcing functions for the dynamic response procedure.

For the transient analysis, several tables are set up so that displacements, reactions, forces and stresses could be followed at points of interest along the structure. Once these tables are created, the modes calculated, and the amplitudes and forces versus time are in the proper form, the dynamic response is initiated and the reactions, displacements, forces and stresses desired are saved versus time.

7.4 Structural Frequencies

Although 80 modes are used in the analysis, the first two modes are the most significant. The first two modes are shown in figure 9.

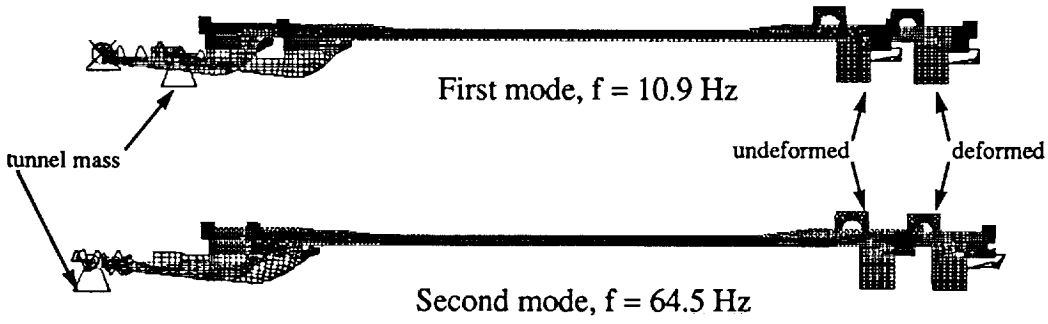

Figure 9. First two Structural Frequencies.

The first mode is 10.9 Hz and is characterized by the stretching of the thrust anchor spring with the tunnel mass and the combustor moving in a rigid body fashion. Therefore, the first mode is the thrust anchor mode. The second mode is 64.5 Hz and is characterized by the stretching of the nozzle and combustor shell with the tunnel mass and the thrust anchor spring remaining stationary. Therefore, the second mode is the nozzle mode.

8.0 Results

The results are shown in tables 9 and 10. Table 9 shows the results for 2.25 kg fuel mass under 10, 50, 100, and 200 m/s flame speeds at 900 psi deflagration pressure. For each of the components, the appropriate criteria is shown for comparison. The controlling component has the value underlined and represents the value used to determine the margin of safety. Table 9 shows that the critical component is the nozzle and that all components have a positive margin of safety. In addition, 10 and 50 m/s have a high margin of safety and the controlling flame speed is 100 m/s.

Table 10 shows the results for 4 kg fuel mass under 100 and 200 m/s flame speeds and 6 and 8 kg fuel mass under 200 m/s flame speed at 900 psi deflagration pressure. Again, the controlling component is the nozzle; but for the nozzle, all cases have a negative margin of safety. In addition, the controlling flame speed is 200 m/s. Therefore from tables 9 and 10, it can be concluded that the allowable fuel mass is between 2.25 and 4 kg and that either 100 or 200 m/s flame speeds can control.

Table 9. Results for 2.25 kg Fuel Mass with varying Flame Speeds.

Component	10 m/s	50 m/s	100 m/s	200 m/s	Failure Criteria
Max Thrust Anchor Load, lbs	7.48×10^{4}	9.41×10^{4}	1.67×10^{5}	2.16×10^{5}	1.00×10^{6}
Max Nozzle Load, lbs	1.44×10^{5}	5.47×10^{5}	1.18×10^{6}	1.07×10^{6}	2.00×10^{6}
Max Hoop Stress, ksi					
Laminate	8.40	9.30	9.75	12.45	93.0
Barrel	5.40	6.00	6.00	7.80	47.0
Max Shear Key Load, lbs					
Closure Plug	2.39×10^{6}	2.65×10^{6}	2.77×10^{6}	3.09×10^{6}	28.3×10^{6}
Nozzle	2.41×10^{6}	2.88×10^{6}	3.36×10^{6}	3.50×10^{6}	28.3×10^{6}
Max Barrel Radial Disp., in					
Closure Plug	.00059	.00083	.00087	.00101	.65
Nozzle	.00053	.00085	.00104	.00110	.65
Max Piping Disp., in					
Combustor Air	.025	.038	.048	.050	2.00
Nozzle Air	.007	.010	.018	.019	.50
Closure Plug Jack Force, lbs	4.05×10^{4}	7.83×10^{4}	9.39×10^{4}	1.61×10^{5}	1.26×10^{6}
Margin of Safety	7.70	2.66	.69	.86	

Table 10. Failure Assessment for Deflagration Loads.

Component	4 kg 100 m/s	4 kg 200 m/s	6 kg 200 m/s	8 kg 200 m/s	Failure Criteria
Max Thrust Anchor Load, lbs	4.78×10^{5}	6.14×10^{5}	9.20×10^{5}	1.25×10^{6}	1.00×10^{6}
Max Nozzle Load, lbs	4.01×10^{6}	5.43×10^{6}	1.05×10^{7}	1.23×10^{7}	2.00×10^{6}
Max Hoop Stress, ksi					
Laminate	14.25	15.15	20.10	24.00	93.0
Barrel	9.60	9.75	14.40	17.25	47.0
Max Shear Key Load, lbs					
Closure Plug	4.90×10^{6}	5.16×10^{6}	8.03×10^{6}	8.87×10^{6}	28.3×10^{6}
Nozzle	6.06×10^{6}	7.72×10^{6}	1.15×10^{7}	1.65×10^{7}	28.3×10^{6}
Max Barrel Radial Disp., in					
Closure Plug	.00159	.00174	.00266	.00283	.65
Nozzle	.00204	.00266	.00403	.00563	.65
Max Piping Disp., in					
Combustor Air	.119	.150	.215	.335	2.00
Nozzle Air	.049	.065	.110	.160	.50
Closure Plug Jack Force	4.17×10^{5}	7.25×10^{5}	8.55×10^{5}	1.10×10^{6}	1.26×10^{6}
Margin of Safety	-.50	-.63	-.81	-.84	

The finite element model dynamic response for the nozzle and thrust anchor is shown in figure 10.

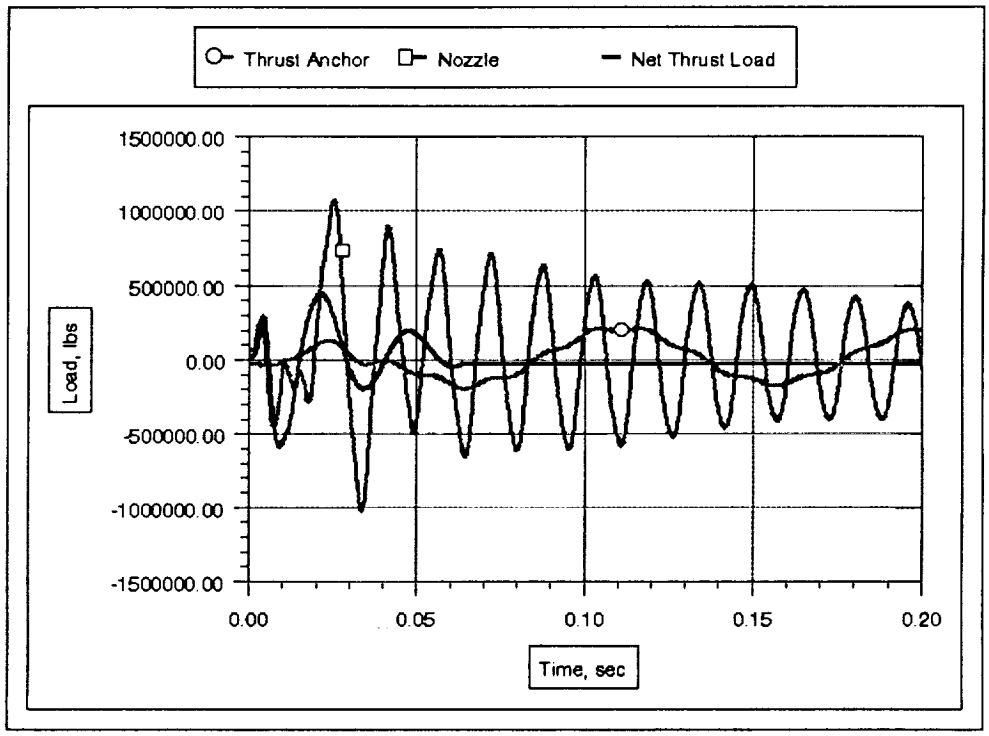

Figure 10. FEM Dynamic Response for 2.25 kg Fuel, 200 m/s Flame Speed @ 900 psi.

In addition, the net thrust load is shown. The results are for 2.25 kg fuel mass, 200 m/s flame speed at 900 psi deflagration pressure. The plot is of load versus time and it shows that the nozzle dynamically responds to the load whereas the thrust anchor is sluggish to respond to the load. The peak nozzle load of 1.07×10^6 lbs occurs at ~.025 seconds and the peak thrust anchor load of 2.16×10^5 lbs occurs at ~.11 seconds. These values are shown in table 9.

8.1 Model Verification.

To verify the results of the FEM analysis, two simple dynamic closed form models were developed. A single degree of freedom model was developed that considered hoop stress due to the radial pressure load. The pressure load used was for 2.25 kg fuel mass, 200 m/s flame speed, at 900 psi initial deflagration pressure. Figure 11 is a plot of the results of the analysis, showing the nozzle end pressure load along with the nozzle end barrel stress versus time. The response is quasi-static with very little dynamic effects. The peak stress is 8.15 ksi as compared to 7.8 ksi for the FEM analysis.

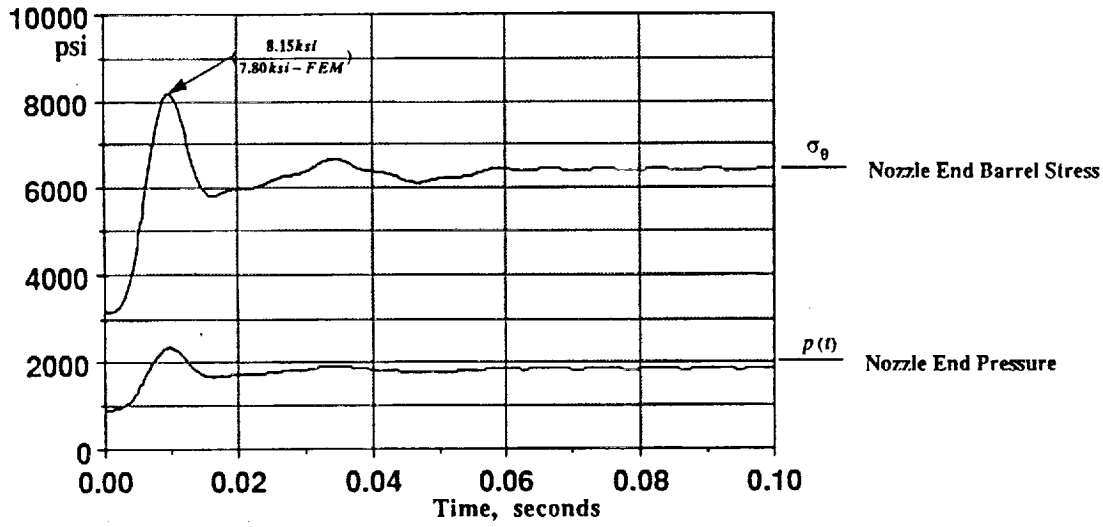

Figure 11. Results from 1-DOF Dynamic Model.

The other model is a three degree of freedom model which incorporates three lumped masses and three springs to determine the effects of the thrust loading. The combustor is modeled as two masses and a spring, the nozzle and the thrust anchor are modeled as springs, and the remaining tunnel is modeled as a lumped mass. The appropriate axial thrust loads are applied to the three masses versus time. The loading used was for 2.25 kg fuel mass, 200 m/s flame speed, at 900 psi initial deflagration pressure. Figure 12 shows the results of the analysis. The plot is of force versus time and includes the applied loads and the response of the nozzle, thrust anchor, and end closure. Three comparisons come from this analysis: (1) the maximum end closure force is 3.18×10^6 as compared to 3.09×10^6 for the FEM analysis, (2) the maximum nozzle force is $.97 \times 10^6$ as compared to 1.07×10^6 for the FEM analysis, and (3) the max thrust anchor force is 1.82×10^6 as

compared to 2.16×10^6 for the FEM analysis. All of the comparisons are good and indicate a high degree of reliability in the FEM analysis.

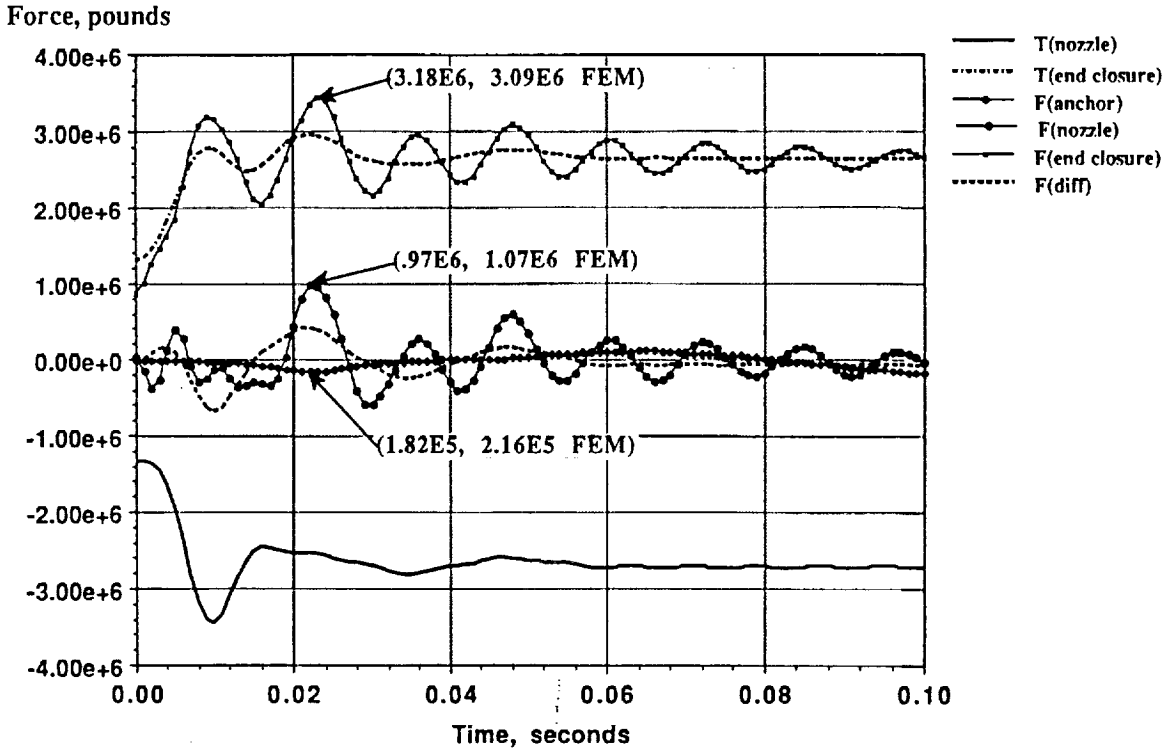

Figure 12. Results from 3-DOF Dynamic Model.

8.2 Frequency Sensitivity

To determine the sensitivity of the structure to the loading transient, structural frequencies were 'tuned' to the loading frequencies (aligning structural frequencies with the dominate load frequencies). To accomplish this, Fast Fourier Transforms (FFT) of the unbalanced loading were performed to determine the dominate load frequencies. Two conditions were considered: (1) the first two structural frequencies were 'tuned' to the dominate frequencies of the pressure loading as a limiting case, and (2) the first two structural frequencies were 'tuned' by 20% to the dominate frequencies of the loading as a design case. Figure 13 shows the FFT of the unbalanced loading for the 2.25 kg fuel, 200 m/s flame speed case. For this case, the first structural frequency was already 'tuned' while the second structural frequency was adjusted as shown in figure 13. This procedure was done for all cases used in the final evaluation.

The results indicate that 'tuning' the structure to the load frequencies consistently made 200 m/s the controlling flame speed. Therefore, all remaining results use a 200 m/s flame speed. Figure 14 is a plot of nozzle load versus deflagration pressure showing the effect of 'tuning' the structural frequencies to the load frequencies. The 2.25kg fuel case is shown 'untuned', 'tuned', and 20% 'tuned'. In addition, the structural response for the 4,

6, 8 kg of fuel load cases are shown along with the allowable nozzle load for comparison.

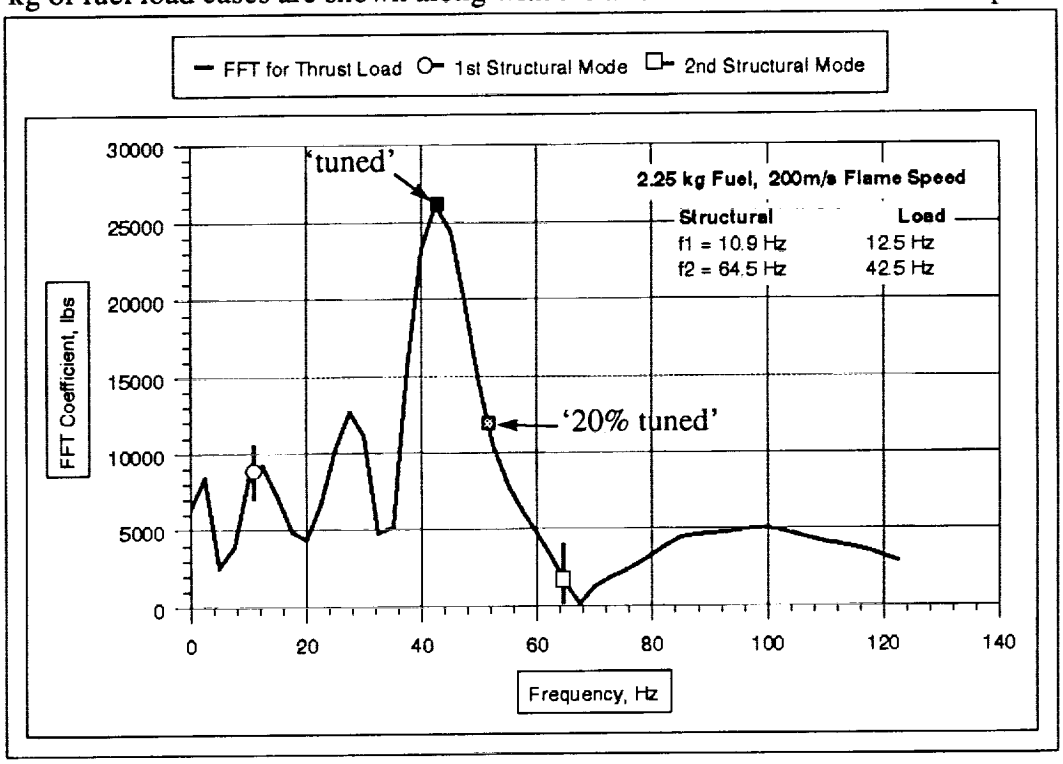

Figure 13. Fast Fourier Transform for Thrust Loading.

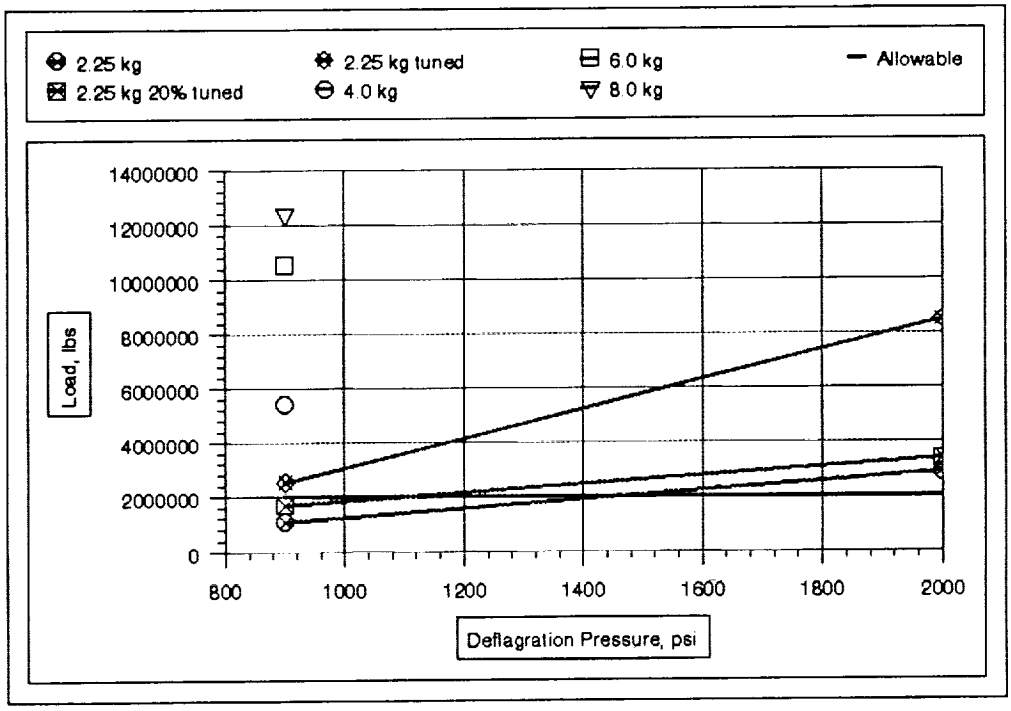

Figure 14. Nozzle Load vs. Deflagration Pressure for Different Fuel Masses.

8.3 Combustor Deflagration Limits.

To determine the combustor deflagration limits, a relationship between equivalent fuel mass and deflagration pressure is determined. To do this, the nozzle load is plotted against equivalent fuel mass for 900, 2000, and 3000 psi initial deflagration pressures which are 20% 'tuned'. Figure 15 shows this plot along with the allowable nozzle load. From this plot, the allowable fuel mass for the three deflagration pressures can be determined where the pressure lines cross the allowable line. Using those three points equivalent fuel mass can be plotted against deflagration pressure as shown in figure 16. Two lines are shown in figure 16; first is the line produced from figure 15 where the allowable nozzle load is used and the system is 20% 'tuned', and second is an upper limit line where the ultimate strength of the nozzle is used and there is no 'tuning'. This results in three different levels of confidence; nozzle OK, marginal, and overloaded.

There is a control system math model which can simulate the combustor processes under various control parameters. The math model can relate equivalent fuel mass to shut down time and deflagration pressure to operating pressure. Therefore, using figure 16 and the control system math model, an allowable shut down time can be determined at a particular operating pressure.

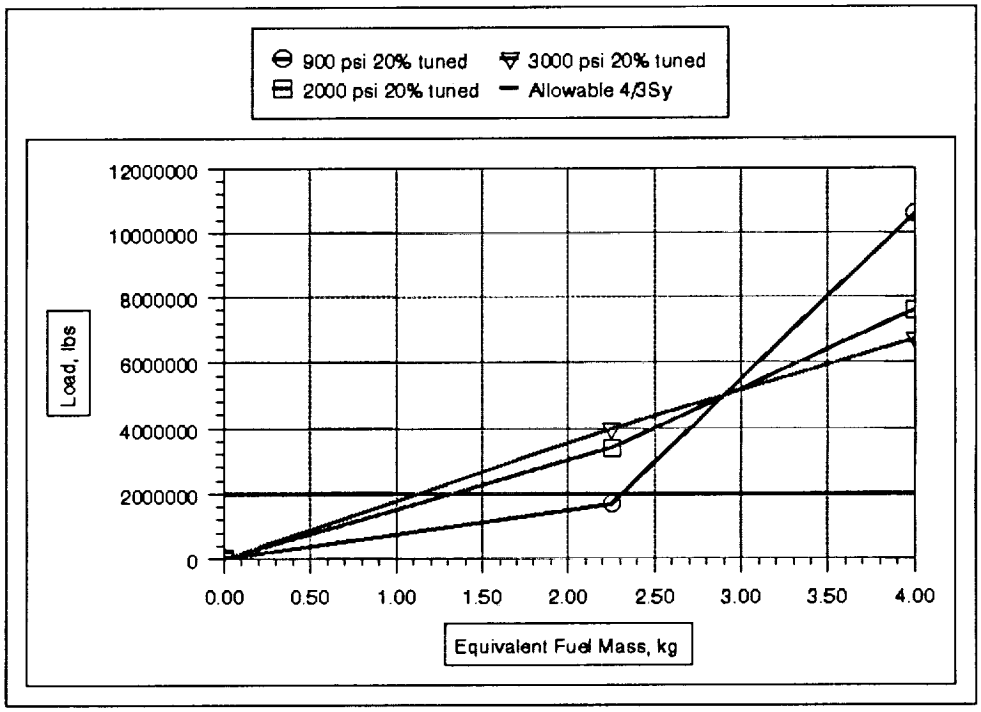

Figure 15. Nozzle Load versus Equivalent Fuel Mass.

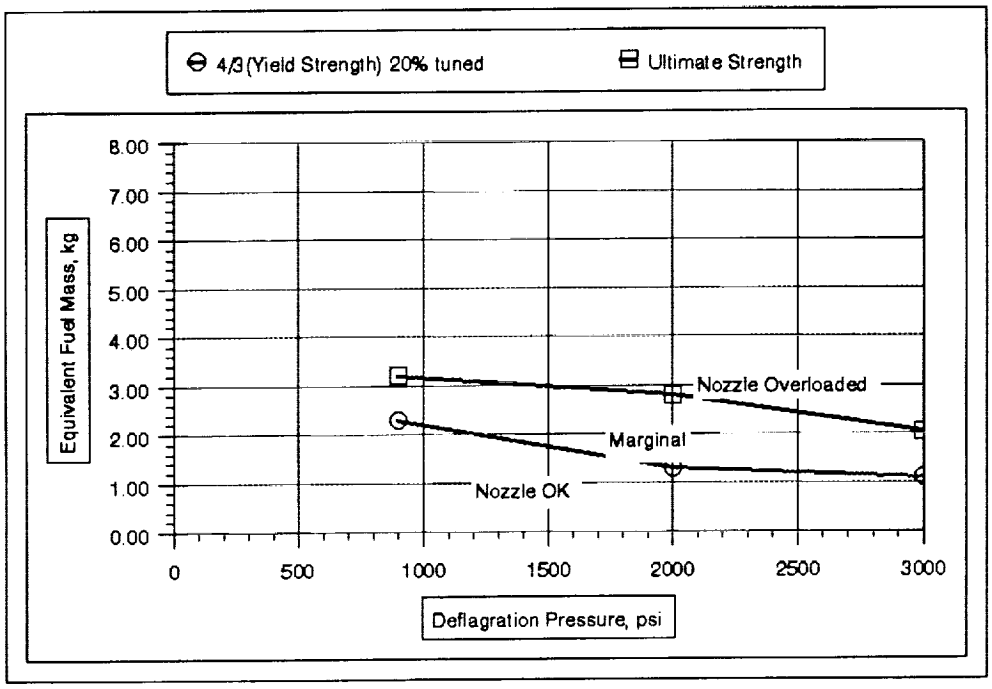

Figure 16. Nozzle Limits for Fuel Mass vs. Deflagration Pressure.

9.0 Conclusions

An analysis has been performed to determine the safe operating limits of the combustor under transient explosive loads. The failure criteria was defined and the failure mechanisms were determined for both peak pressure and differential pressure loadings. An overview of the gas dynamics analysis was given. The overview indicates that for methane-air operation, there is not a sufficient ignition source to initiate a detonation and a DDT is improbable because flame speed will not accelerate sufficiently with an increase in pressure. Therefore only a deflagration is possible under methane-air operation. For methane-O_2 operation, flame speed can accelerate from a deflagration into a detonation. Therefore, a deflagration and a DDT are possible for methane-LOX operation. Preliminary assessments indicated that the combustor could not safely contain any level of a DDT and that the combustor can only safely contain a low-level deflagration. Therefore, the main consideration in this analysis was to determine the maximum level of deflagration that the structure could withstand.

A finite element model of the end closure plug, pressure shell, combustor nozzle, tunnel mass and thrust anchor was constructed to evaluate 13 transient load cases. To assess the sensitivity of the structure to the frequency content of the transient loading, structural frequencies were 'tuned' to the loading frequencies. In addition, two closed form dynamic analyses were conducted to verify the finite element analysis with excellent correlation. It was determined that the differential pressure load or thrust load was the critical load mechanism and that the nozzle is the weak link in the combustor system.

REFERENCES

1. PATRAN Division/PDA Engineering, PATRAN Plus Users Manual Vol. 1 and 2, July 1988.

2. Whetstone, W. D., EISI-EAL Engineering Analysis Language Reference Manual, EISI-EAL System Level 312. Engineering Information Systems, Inc., August 1985.

3. Chu-Kia Wang and Charles G. Salmon. Reinforced Concrete Design, Third Edition, Harper & Row, 1979.

4. Numerical Computation of Blast Waves in the NASA LaRC 8' HTT Combustor, Arthur D. Little, Cambridge, Report to PRC, March 4, 1991.

5. Kuchta, US Bureau of Mines Bulletin 680, 1985.

6. M. G. Zabetakis. Flammability Characteristics of Combustible Gases and Vapors. US Bureau of Mines Bulletin 627, 1965.

7. Bradley, D. and Mitcheson, A. The Venting of Gaseous Explosions in Spherical Vessels. II-Theory and Experiment, Combustion and Flame 32, 237-255, 1978

8. Reynolds, W. C. The Element Potential Method for Chemical Equilibrium Analysis: Implementation in the Interactive Program STANJAN, Version 3 Dept. of Mechanical Engineering, Stanford, CA, January 1986.

REPORT DOCUMENTATION PAGE

Form Approved
OMB No. 0704-0188

1. AGENCY USE ONLY (Leave blank)	2. REPORT DATE	3. REPORT TYPE AND DATES COVERED
	December 1992	Technical Memorandum

4. TITLE AND SUBTITLE

Transient/Structural Analysis of a Combustor Under Explosive Loads

5. FUNDING NUMBERS

WU 505-43-31-05

6. AUTHOR(S)

Peyton B. Gregory and Anne D. Holland

7. PERFORMING ORGANIZATION NAME(S) AND ADDRESS(ES)

NASA Langley Research Center
Hampton, VA 23681-0001

8. PERFORMING ORGANIZATION REPORT NUMBER

9. SPONSORING/MONITORING AGENCY NAME(S) AND ADDRESS(ES)

National Aeronautics and Space Administration
Washington, DC 20546-0001

10. SPONSORING/MONITORING AGENCY REPORT NUMBER

NASA TM-107660

11. SUPPLEMENTARY NOTES

12a. DISTRIBUTION/AVAILABILITY STATEMENT

Unclassified - Unlimited
Subject Category - 39

12b. DISTRIBUTION CODE

13. ABSTRACT (Maximum 200 words)

The 8-Foot High Temperature Tunnel (HTT) at NASA Langley Research Center is a combustion-driven blow-down wind tunnel. A major potential failure mode that was considered during the combustor redesign was the possibility of a deflagration and/or detonation in the combustor. If a main burner flame-out were to occur, then unburned fuel gases could accumulate and, if reignited, an explosition could occur. An analysis has been performed to determine the safe operating limits of the combustor under transient explosive loads. The failure criteria was defined and the failure mechanisms were determined for both peak pressure and differential pressure loadings. An overview of the gas dynamics analysis was given. A finite element model was constructed to evaluate 13 transient load cases. The sensitivity of the structure to the frequency content of the transient loading was assessed. In addition, two closed form dynamic analyses were conducted to verify the finite element analysis. It was determined that the differential pressure load or thrust load was the critical load mechanism and that the nozzle is the weak link in the combustor system.

14. SUBJECT TERMS

Structural Analysis
Finite Element Analysis
Combustor
Explosive Loads

15. NUMBER OF PAGES

26

16. PRICE CODE

A03

17. SECURITY CLASSIFICATION OF REPORT	18. SECURITY CLASSIFICATION OF THIS PAGE	19. SECURITY CLASSIFICATION OF ABSTRACT	20. LIMITATION OF ABSTRACT
Unclassified	Unclassifed	Unclassified	UL